Reconstruction of the murine extrahepatic biliary tree using primary
 human extrahepatic cholangiocyte organoids.

3

Fotios Sampaziotis^{1,2,3}, Alexander W Justin⁴, Olivia C. Tysoe^{1,2}, Stephen 4 Sawiak^{5†}, Edmund M Godfrey^{6†}, Sara S Upponi^{6†}, Richard L. Gieseck III⁷, 5 Miguel Cardoso de Brito^{1,2}, Natalie Lie Berntsen⁸, María J Gómez-Vázguez⁹, 6 Daniel Ortmann^{1,2}, Loukia Yiangou^{1,10,11}, Alexander Ross^{1,12,13}, Johannes 7 Bargehr^{1,10,11,14}, Alessandro Bertero^{1,2}, Mariëlle CF Zonneveld¹, Marianne T 8 Pedersen¹⁵, Matthias Pawlowski¹, Laura Valestrand⁸, Pedro Madrigal^{1,16}, 9 Nikitas Georgakopoulos², Negar Pirmadjid², Gregor M Skeldon^{17,18}, John 10 Casey¹⁹, Wenmiao Shu^{17,18}, Paulina M Materek²⁰, Kirsten E Snijders¹, 11 Stephanie E Brown^{1,2}, Casey A Rimland^{1,2,7,21}, Ingrid Simonic²², Susan E 12 Davies²³, Kim B Jensen¹⁵, Matthias Zilbauer^{10,12,13}, William TH Gelson³, 13 Graeme Alexander¹¹, Sanjay Sinha^{1,14}, Nicholas RF Hannan^{24,25}, Thomas A 14 Wynn⁷, Tom H Karlsen⁸, Espen Melum⁸, Athina E. Markaki⁴, Kourosh Saeb-15 Parsv²*. Ludovic Vallier^{1,2,10,16}* 16

17

¹Wellcome Trust-Medical Research Council Stem Cell Institute, Cambridge
 Stem Cell Institute, Anne McLaren Laboratory, University of Cambridge,
 Cambridge, UK

²Department of Surgery, University of Cambridge and NIHR Cambridge
 Biomedical Research Centre, Cambridge, UK

²³ ³Department of Hepatology, Cambridge University Hospitals NHS Foundation

24 Trust, Cambridge, UK

⁴Department of Engineering, University of Cambridge, Cambridge, UK 1 ⁵Department of Clinical Neurosciences, University of Cambridge, Cambridge, 2 UK 3 ⁶Department of Radiology, Cambridge University Hospitals NHS Foundation 4 Trust, Cambridge, UK 5 ⁷Immunopathogenesis Section, Laboratory of Parasitic Diseases, National 6 Institute of Allergy and Infectious Diseases, National Institutes of Health. 7 Bethesda, Maryland, USA 8 ⁸Norwegian PSC Research Center, Department of Transplantation Medicine, 9 Division of Surgery, Inflammatory Diseases and Transplantation, Oslo 10 University Hospital, Rikshospitalet, Oslo. 11 ⁹Cambridge Genomic Services, Department of Pathology, University of 12 Cambridge, Cambridge, UK 13 ¹⁰Wellcome Trust-Medical Research Council Stem Cell Institute, Cambridge 14 Stem Cell Institute, University of Cambridge, Cambridge, UK 15 ¹¹Department of Medicine, School of Clinical Medicine, University of 16 Cambridge, Cambridge, UK. 17 ¹²University Department of Paediatrics, University of Cambridge, Cambridge, 26 UK 27 ¹³Department of Paediatric Gastroenterology, Hepatology and Nutrition, 28 Cambridge University Hospitals NHS Foundation Trust, Cambridge, UK 29 ¹⁴Division of Cardiovascular Medicine, University of Cambridge, Cambridge, 30 UK 31 ¹⁵Biotech Research and Innovation Centre (BRIC), University of Copenhagen, 32 Copenhagen, Denmark 33

- ¹⁶Wellcome Trust Sanger Institute, Hinxton, UK
- ¹⁷School of Engineering and Physical Sciences, Heriot-Watt University, United
- 3 Kingdom
- ⁴ ¹⁸Department of Biomedical Engineering, University of Strathclyde, United
- 5 Kingdom
- ⁶ ¹⁹Department of Surgery, University of Edinburgh, Edinburgh Royal Infirmary,
- 7 Edinburgh, EH16 4SU, United Kingdom
- 8 ²⁰NIHR Cambridge Biomedical Centre (BRC) hIPSCs core facility
- ⁹ ²¹University of North Carolina, Chapel Hill School of Medicine, Chapel Hill,
- 10 North Carolina, USA
- ²²Medical Genetics Laboratories, Cambridge University Hospitals NHS Trust,
- 12 Cambridge, UK
- ¹³²³Department of Histopathology, Cambridge University Hospitals NHS
- 14 Foundation Trust, Cambridge, UK
- ²⁴Center for Biomolecular Sciences, University of Nottingham, UK
- ²⁵Nottingham Digestive Diseases Centre, National Institute for Health
- 17 Research (NIHR) Nottingham Biomedical Research Centre at the Nottingham

18 University Hospitals NHS Trust and University of Nottingham.

- 19
- Authorship note: * Kourosh Saeb-Parsy and * Ludovic Vallier contributed equally to this work.
- [†]Stephen Sawiak, [†]Edmund Godfrey and [†]Sara Upponi contributed equally to
 this work.
- Correspondence: Ludovic Vallier, Laboratory for Regenerative Medicine,
 West Forvie Building, Robinson Way, University of Cambridge. Cambridge

- CB2 0SZ, United Kingdom. Telephone: 44.1223.747489; Fax:
 44.1223.763.350; E-mail: <u>lv225@cam.ac.uk</u>.
- 3
- 4 Keywords: Cholangiocytes, bile duct, bio-engineering, tissue engineering,
- 5 organoids, regenerative medicine, cell-based therapy, biliary atresia, PGA
- 6 scaffold, collagen scaffold, densified collagen
- 7

1 Abstract

2	Treatment of common bile duct disorders such as biliary atresia or ischaemic
3	strictures is limited to liver transplantation or hepatojejunostomy due to the
4	lack of suitable tissue for surgical reconstruction. Here, we report a novel
5	method for the isolation and propagation of human cholangiocytes from the
6	extrahepatic biliary tree and we explore the potential of bioengineered biliary
7	tissue consisting of these extrahepatic cholangiocyte organoids (ECOs) and
8	biodegradable scaffolds for transplantation and biliary reconstruction in vivo.
9	ECOs closely correlate with primary cholangiocytes in terms of transcriptomic
10	profile and functional properties (ALP, GGT). Following transplantation in
11	immunocompromised mice ECOs self-organize into tubular structures
12	expressing biliary markers (CK7). When seeded on biodegradable scaffolds,
13	ECOs form tissue-like structures retaining biliary marker expression (CK7)
14	and function (ALP, GGT). This bioengineered tissue can reconstruct the wall
15	of the biliary tree (gallbladder) and rescue and extrahepatic biliary injury
16	mouse model following transplantation. Furthermore, it can be fashioned into
17	bioengineered ducts and replace the native common bile duct of
18	immunocompromised mice, with no evidence of cholestasis or lumen
19	occlusion up to one month after reconstruction. In conclusion, ECOs can
20	successfully reconstruct the biliary tree following transplantation, providing
21	proof-of-principle for organ regeneration using human primary cells expanded
22	<mark>in vitro.</mark>

Disorders of the extrahepatic bile ducts carry considerable morbidity and 1 mortality. Indeed, 70% of pediatric liver transplantations are performed to treat 2 biliary atresia¹, Primary Sclerosing Cholangitis (PSC) alone accounts for 5% 3 of US liver transplantations² and biliary complications are the leading cause of 4 graft failure following deceased liver transplantation^{3,4}. Treatment options 5 remain limited^{5,6} due to the lack of healthy tissue that can be used to 6 reconstruct and replace diseased bile ducts. In vitro expansion of native 7 cholangiocytes could address this challenge and provide cells suitable for 8 9 tissue engineering applications such as biliary reconstruction. However, the culture of primary biliary epithelium remains problematic⁷. Here we report a 10 novel method for the isolation and propagation of primary human 11 12 cholangiocytes from the extrahepatic biliary tree, compatible with regenerative medicine applications. The resulting Extrahepatic Cholangiocyte Organoids 13 (ECOs) express key biliary markers such as Cytokeratin 7 (KRT7 or CK7), 14 15 Cytokeratin 19 (KRT19 or CK19), Gamma Glutamyl-Transferase (GGT), Cystic fibrosis transmembrane conductance regulator (CFTR) and maintain 16 their functional properties in vitro including Alkaline Phosphatase (ALP), GGT 17 activity and responses to secretin and somatostatin. The potential of ECOs for 18 tissue engineering and clinical applications is further illustrated by their 19 20 capacity to populate biodegradable scaffolds, organize into a functional biliary epithelium and rescue a murine model of extrahepatic biliary injury (EHBI). 21

22

23 **Results**

24 Human extrahepatic cholangiocytes can be propagated as organoids

We first focused on identifying optimal conditions to isolate primary 1 cholangiocytes from the biliary epithelium which forms a monolayer covering 2 the luminal surface of the biliary tree⁸. We tested several approaches for 3 recovering these cells and mechanical dissociation by brushing or scraping 4 the bile duct lumen was associated with improved survival compared to 5 enzymatic digestion (Figure 1a, Supplementary Fig 1a). Furthermore, the 6 7 majority of the resulting cells co-expressed the biliary markers CK7 and CK19 $(94.6 \pm 2.4\%, SD; n=3)$; while no contamination from mesenchymal cell types 8 9 was detected (Supplementary Fig 2). Consequently, mechanical dissociation constitutes the optimal method for harvesting extrahepatic cholangiocytes. 10

11 To discern appropriate conditions for the maintenance and propagation of these cells, we optimized our recently established system for 3D culture of 12 human induced pluripotent stem cell-derived intrahepatic cholangiocytes^{9,10}. 13 Screening of multiple growth factors known to support expansion of 14 cholangiocytes and epithelial organoids^{11,12} (Supplementary Fig 1b-1c) 15 identified that the combination of Epidermal Growth Factor (EGF), R-spondin 16 and Dickkopf-related protein 1 (DKK-1) promoted the growth of primary 17 18 cholangiocytes into organoids (Supplementary Fig 3a, 3b). Due to the paradoxical requirement for both a Wnt potentiator (R-spondin) and an 19 inhibitor (DKK-1), we characterized the canonical and non-canonical/PCP Wnt 20 pathway activity in ECOs. Our results demonstrate higher β-catenin 21 phosphorylation in ECOs compared to cells treated with R-spondin but no 22 DKK-1 (Supplementary Fig 1d-1e), signifying lower WNT canonical pathway 23 activity in these cells. Furthermore ECOs exhibit higher Rho Kinase activity 24 compared to cells treated with R-spondin but no DKK-1 (Supplementary Fig 25

1 f), which could be consistent with enhanced non-canonical/PCP signaling in
ECOs. Thus, it is possible that non-canonical Wnt signaling controls ECO
expansion marking a notable difference with previous organoid culture
conditions¹².

Under these conditions, we derived 8 different ECO lines (Supplementary 5 Table 1) from a variety of deceased donors aged from 33 to 77 years. 6 Notably, we obtained similar results by using cholangiocytes isolated from the 7 gallbladder or by harvesting common bile duct cholangiocytes using an 8 Endoscopic Retrograde Cholangio-Pancreatography (ERCP) brush instead of 9 10 scrapping the lumen (Supplementary Fig 4). Consequently, ECOs can be 11 derived from different areas of the extra-hepatic biliary tree and harvested using peri-operative (dissection and scrapping) or minimally invasive (ERCP 12 brushings) approaches. 13

14

15 ECOs maintain key biliary markers and function in culture

The resulting cells were expanded in vitro for prolonged periods of time 16 while (Supplementary Fig 5a) maintaining their genetic stability 17 (Supplementary Fig 5b-5c). Electron microscopy revealed the presence of 18 characteristic ultrastructural features including cilia, microvilli and tight 19 junctions¹³ (Supplementary Fig 3c), while QPCR and immunofluorescence 20 21 (IF) analyses established the expression of key biliary markers such as KRT7 or CK7, KRT19 or CK19, Hepatocyte Nuclear Factor 1 beta (HNF1B), GGT, 22 Secretin Receptor (SCTR), sodium-dependent bile acid transporter 23 (ASBT/SLC10A2), CFTR and SRY-box 9 (SOX9)⁹ (Figure 1b-1c. 24

Supplementary Fig 4c-4d, 3d-3e). Of note, stem cell markers such as 1 POU5F1 or OCT4, NANOG, prominin 1 (PROM1), leucine rich repeat 2 containing G protein-coupled receptor (LGR) LGR-4/5/6; markers of non-3 biliary lineages including albumin (ALB), α1-antitrypsin (SERPINA1 or A1AT), 4 keratin 18 (KRT18), pancreatic and duodenal homeobox 1 (PDX1), insulin 5 (INS) and glucagon (GCG); and EMT markers (vimentin (VIM), snail family 6 7 transcriptional repressor 1 (SNAI1) and S100 calcium binding protein A4 (S100A4) were not detected (Supplementary Fig 6a-6c). On the other hand, 8 9 98.1% ± 0.9% (SD; n=3) of the cells co-expressed CK7 and CK19 following 20 passages (Supplementary Fig 2) thereby confirming the presence of a 10 near homogeneous population of cholangiocytes. 11

Transcriptomic analyses (Figure 1d, Supplementary Fig 7, Supplementary 12 Table 2) revealed that ECOs maintain a stable gene expression profile over 13 multiple passages (Pearson correlation coefficient for Passage 1 (P1) vs. 14 Passage 20 (P20) r=0.99, Supplementary Fig 7a-b), express key biliary 15 markers (Supplementary Fig 7c) and cluster closely to freshly isolated 16 cholangiocytes (Supplementary Fig 7d) (Pearson correlation coefficient for 17 18 Primary Cholangiocytes (PCs) vs. Passage 20 (P20) r=0.92; Supplementary Fig 7b). Gene ontology analyses confirmed enrichment of pathways 19 characteristic for the biliary epithelium (Supplementary Fig 7e). Considered 20 collectively, these results demonstrate that primary cholangiocytes derived 21 from the extrahepatic biliary tree can be expanded in vitro without losing their 22 original characteristics. 23

We then further characterized ECOs by focusing on their function following long term culture (20 passages). The biliary epithelium regulates the

homeostasis of bile through the transport of ions, water and bile acids^{8,14}. The 1 secretory capacity of ECOs was interrogated using Rhodamine-123, a 2 fluorescent substrate for the cholangiocyte surface glycoprotein Multidrug 3 (MDR1)^{15,16} Resistance protein-1 (Figure 2a-2c). Rhodamine-123 4 accumulated in the ECO lumen only in the absence of the MDR-1 antagonist 5 verapamil, thereby confirming active secretion through MDR-1 (Figure 2a-2c). 6 Luminal extrusion of bile acids¹⁷ was also demonstrated by showing that the 7 fluorescent bile acid Cholyl-Lysyl-Fluorescein (CLF) was actively exported 8 9 from ECOs (Figure 2d-2f). Furthermore, ECO ALP and GGT activity was comparable to freshly plated primary cholangiocytes (Figure 2g-2h, 10 Supplementary Fig 4e-4f). The response of ECOs to secretin and 11 somatostatin was also assessed. Secretin promotes water secretion, 12 distending the bile duct lumen, while somatostatin negates the effects of 13 secretin¹⁸⁻²⁰. Accordingly, organoids exposed to secretin increased their 14 15 diameter compared to untreated controls, while somatostatin inhibited the effect of secretin (Figure 2i-2j). Our data, therefore, demonstrate that ECOs 16 maintain their functional properties after long term culture. 17

18

19 ECOs self-organize into tubular structures after transplantation

These results prompted us to investigate the potential of ECOs for in vivo use, especially regenerative medicine applications. We first characterized the potential of ECOs for in vivo engraftment and survival by transplanting cells under the kidney capsule of NOD.Cg-Prkdc^{scid} II2rg^{tm1WjI} (NSG) mice (Supplementary Fig 8a) for 12 weeks²¹. ECOs successfully engrafted forming

tubular structures expressing biliary markers such as CK19 (Supplementary
Fig 8b-d).

Notably, no tumour formation or markers of differentiation to other lineages
were detected (Supplementary Fig 8d). Thus, ECOs appear to maintain their
basic characteristics even after prolonged engraftment in vivo under the
kidney capsule.

7

8 **ECOs populate biodegradable scaffolds**

To assess the potential of ECOs for tissue engineering, we first interrogated 9 10 their capacity for populating Polyglycolic Acid (PGA) biodegradable scaffolds commonly used to provide the structural and mechanical support required for 11 tissue reconstruction²². Indeed, PGA is one of the most widely used synthetic 12 polymers since it does not induce inflammatory responses in the surrounding 13 tissue; it is biodegradable; and it is more flexible and easier to process 14 compared to natural polymers such as collagen²³. To facilitate tracking of the 15 cells, ECOs expressing Green Fluorescent Protein (GFP) were generated 16 through viral transduction (Supplementary Fig. 9a-9b). The resulting cells 17 were seeded on PGA scaffolds, attached to the PGA fibers after 24-48 hours 18 and continued to grow for 4 weeks until the scaffold was confluent (Figure 3a-19 3d). Primary cholangiocytes plated in 2D conditions demonstrated limited 20 expansion potential and failed to reach confluency when seeded on the 21 scaffolds (Supplementary Fig 10a-b), suggesting that the proliferative capacity 22 of ECOs is crucial for successful scaffold colonization. The populated PGA 23 scaffolds (Figure 3b-3c), could easily be handled with forceps and divided into 24

smaller pieces with a surgical blade. Furthermore, the cells populating the scaffolds retained expression of biliary markers such as CK7 and CK19 (Figure 3e-3f), demonstrated no evidence of epithelial–mesenchymal transition (EMT; Figure 3e, 3g) and maintained their functional properties including ALP and GGT activity (Figure 3h-3i). Therefore, ECOs can successfully populate PGA scaffolds, while maintaining their functionality and marker expression.

8

9 ECO-populated scaffolds reconstruct the gallbladder wall

Following these encouraging results, we decided to define the capacity of 10 ECOs to repair the biliary epithelium. For that, we developed a mouse model 11 12 of extrahepatic biliary injury (EHBI). More specifically, to simulate biliary tree wall defects requiring biliary reconstruction²⁴, the biliary tree of healthy NSG 13 mice was compromised through a longitudinal incision in the gallbladder wall 14 (Figure 4a). The surgical defect in the gallbladder wall was subsequently 15 repaired by transplanting bioengineered tissue into the injured animals, which 16 17 was generated using GFP-expressing ECOs (see previous section; Figure 3). Acellular PGA scaffolds and scaffolds populated with GFP-expressing 18 19 fibroblasts (Supplementary Fig 11a-11d) were used as a negative controls. Animals receiving acellular scaffolds died within 24 hours of the operation 20 (Figure 4b) and post-mortem examination revealed yellow pigmentation of the 21 peritoneal cavity and seminal vesicles consistent with bile 22 leak 23 (Supplementary Fig 12a); while all animals in the fibroblast-scaffold group failed to reconstruct their gallbladder which was replaced by fibrotic tissue 24

incompatible with bile transport or storage (Supplementary Fig 13e-13g). In 1 contrast, animals transplanted with scaffolds containing ECOs survived for up 2 to 104 days without complications and were culled electively (Figure 4b). 3 Notably, the reconstructed gallbladders in the ECO group were fully 4 remodeled resembling the morphology of their native counterparts (Figure 4c, 5 Supplementary Fig 12b). Histology (Figure 3d), IF and QPCR analyses of the 6 7 ECO-reconstructed gallbladders (Figure 3e, Supplementary Fig 14c-14d) unveiled integration of GFP-positive ECOs expressing biliary markers, such 8 9 as KRT19, KRT7, HNF1B, SOX9, CFTR and a human-specific epitope for Ku80 (Figure 4e, Supplementary Fig 12c). Of note, these IF analyses also 10 showed the presence of mouse mesenchymal cells expressing vimentin and 11 12 endothelial cells expressing CD31 in the reconstructed biliary epithelium suggesting that the scaffold is colonized by endogenous cells after 13 transplantation (Supplementary Fig 12c). Furthermore, we also identified a 14 15 population of GFP+/vimentin+/CK19- cells, suggesting that ECOs may also contribute to the scaffold stroma in vivo; possibly through EMT 16 (Supplementary Fig 12c, 12e). The integrity of the reconstructed gallbladder 17 lumen and its exposure to bile through continuity with the biliary tree were 18 demonstrated using Magnetic Resonance Cholangio-Pancreatography 19 20 (MRCP) imaging prior to removal of the organ and was further confirmed with FITC cholangiograms (Figure 4f-4g, Supplementary Fig 12f, Supplementary 21 Video 1). Post mortem surgical examination and full body Magnetic resonance 22 23 Imaging 104 days post transplantation revealed no evidence of tumor formation (Supplementary Fig 12f, Supplementary Video 2) while IF analyses 24 revealed no GFP+ cells in the adjacent liver tissue (data not shown). On the 25

1 contrary, gallbladders reconstituted with fibroblasts controls exhibited 2 obliteration of the gallbladder lumen (Supplementary Fig 11h-11i) and 3 replacement of the lumen and biliary epithelium by fibroblasts expressing 4 Fibroblast Specific Antigen S100A4 (Supplementary Fig. 11i-11j). Considered 5 collectively, our findings demonstrate the capacity of ECOs to colonize their 6 physiological niche and regenerate part of the biliary tree without any 7 complications.

8

9 ECOs on collagen scaffolds generate bioengineered bile ducts

Reconstruction of the gallbladder wall provided proof-of-principle for the 10 capacity of ECOs to regenerate the biliary epithelium after injury; however, the 11 majority of extrahepatic bile duct disorders affect the common bile duct (CBD). 12 Therefore, we focused on the generation of a tubular ECO-populated scaffold, 13 which could be used for bile duct replacement surgery. The internal diameter 14 of the mouse CBD is approximately 100µm with a wall thickness of less than 15 50µm, which precluded the use of a PGA scaffold due to mechanical 16 17 properties. Instead, we generated densified collagen tubular scaffolds (Figure 5a-5b) which were populated with GFP-expressing ECOs (Figure 5c-5e). The 18 use of densified collagen enabled the generation of constructs with an 19 external diameter ranging from 250 to 600µm and adequate strength to 20 maintain a patent lumen (Figure 5d). Notably, the cells populating the collagen 21 scaffolds maintained expression of biliary markers such as KRT19, KRT7, 22 HNF1B, SOX9 and CFTR (Figure 5f-5g) and exhibited GGT and ALP 23 enzymatic activity (Figure 5h-5i). Primary epithelial cells of different origin 24

1	(human mammary epithelial cells; HMEC) failed to survive and adequately
2	populate densified collagen tubes under the same conditions (Supplementary
3	Fig. 13a). Moreover, plated HMECs failed to survive in a 10% (vol/vol) bile
4	solution compared to ECOs (Supplementary Fig. 13b), further confirming that
5	ECOs constitute the only cell type capable of generating bile resistant bio-
6	engineered bile ducts. Collectively, these results demonstrate the capacity of
7	ECOs for populating tubular densified collagen scaffolds without losing their
8	original characteristics.

9

10 Bioengineered bile ducts replace the native mouse bile duct

We then decided to explore the possibility to replace the native CBD of NSG 11 mice with a bioengineered duct consisting of an ECO-populated densified 12 collagen tube (Figure 5). A mid-portion of the native CBD was removed and 13 an ECO-populated collagen tube was anastomosed end-to-end to the 14 proximal and distal duct remnants (Figure 6a). Fibroblast populated tubes 15 were used as a negative control. Biliary reconstruction was achieved in all 16 17 animals transplanted with ECO-populated tubes (Figure 6b-6c, Supplementary Fig 14a-14d), which were followed up for up to a month post 18 transplantation (Supplementary Fig 14d). Histology and IF and QPCR 19 20 analyses (Figure 6d-6f, Supplementary Fig 14a-14b) revealed a patent lumen, with formation of a biliary epithelium by the transplanted GFP+ cells (Figure 21 6e-6f, Supplementary Fig 14a-14b); confirmed the expression of biliary 22 23 markers, such as KRT19, KRT7, HNF1B, CFTR, SOX9 (Figure 6d, 6f, Supplementary Fig 14b) by the engrafted cells; but also illustrated the 24

presence of mouse stromal and endothelial cells (Supplementary Fig 14b). 1 Moreover, we observed minimal apoptosis and proliferation in the 2 3 transplanted tubes 1 month after transplantation, confirming the stability and integrity of the reconstituted biliary epithelium (Supplementary Fig 14b-14c). 4 Lumen patency was further confirmed by Fluorescein Isothiocyanate (FITC) 5 cholangiogram, MRCP and serum cholestasis marker measurements (Figure 6 7 6g, Supplementary Fig 14e-14f, Supplementary video 3). Accordingly animals receiving ECO-populated tubes exhibited no elevation in serum cholestasis 8 9 markers (Bilirubin, ALP; Supplementary Fig 14e) and a patent lumen on imaging (Figure 6g, Supplementary Fig 14f); while the bio-artificial common 10 bile ducts retained their ALP activity in vivo (Figure 6h). 11

On the contrary, all fibroblast-populated collagen tubes failed due to lumen occlusion (Figure 6b-6c, 6e-6g, Supplementary Fig 14d), resulting in high biliary pressures and bile leak through the site of anastomosis (Figure 6b). In conclusion, our results demonstrate the capacity of ECO-populated collagen tubes to replace the native CBD in vivo.

17

18 Discussion

We have demonstrated that epithelial cells from the extrahepatic biliary tree can be expanded and propagated in vitro while maintaining their cholangiocyte transcriptional signature and functional characteristics. In addition, our results show that primary cholangiocytes expanded in vitro as organoids have a unique potential for organ regeneration. Indeed, our system provides the first proof-of-principle for the application of regenerative medicine

in the context of common bile duct pathology. The capacity to replace a
diseased common bile duct with an in vitro bio-engineered ECO-tube could
have a considerable impact for the management of disorders such as biliary
atresia, which constitutes the leading cause for pediatric liver transplantation¹;
or ischemic strictures which are one of the most common complications
following transplantation³. Consequently ECO-populated scaffolds constitute a
novel system with high clinical relevance in the field of cholangiopathies.

Furthermore, studies of the extrahepatic biliary epithelium have been limited 8 by technical challenges in long-term culture and large-scale expansion of 9 10 primary cholangiocytes. These challenges have so far precluded large scale experiments such as transcriptomic and genome-wide analyses which are 11 urgently needed to better understand bile duct diseases, such as PSC and 12 13 cholangiocarcinoma. The capacity of ECOs for large scale expansion, could address this challenge. Indeed, we demonstrate that starting from 10⁵ 14 extrahepatic cholangiocytes we can generate between $10^{20} - 10^{25}$ cells after 15 20 passages. Therefore, ECOs not only represent a novel source of cells for 16 cell based therapy but also provide a unique model system for studying the 17 physiology and modeling disorders of the extrahepatic biliary tree in vitro. 18

Access to human tissue constitutes a considerable limitation for systems 19 based on primary cells. However, we show that ECOs can be obtained not 20 only from the common bile duct but also from the gallbladder. Gallbladder 21 22 tissue is easily accessible and routinely discarded following liver transplantation and cholecystectomy, one of the most common surgical 23 procedures performed. Furthermore, in individuals not having surgery the 24 25 common bile duct can be accessed using minimally invasive procedures, such

as Endoscopic Retrograde Cholangio-Pancreatography (ERCP) and we 1 demonstrate that cholangiocytes can be obtained through brushings, which 2 are routinely performed to acquire histology specimens. Notably, no 3 morphological or functional differences were observed between organoids 4 obtained with these different methods. Moreover, due to the scalability of our 5 system only a small amount of starting material is required. Finally, recent 6 progress in replacing Matrigel by custom made hydrogels to grow gut 7 organoids²⁵ suggest that translating our system from Matrigel to Good 8 9 Manufacturing Practice (GMP) could be feasible. Considered together, these approaches effectively address challenges of tissue availability and open the 10 possibility of autologous as well as allogeneic cell based therapy. 11

Notably, the derivation of primary hepatic stem cells using an organoid culture 12 system has been reported previously¹². However, the capacity of the resulting 13 cells to differentiate into functional cholangiocytes and populate the biliary tree 14 in vivo remains to be demonstrated. Furthermore, in vivo applications of such 15 platforms could be restricted by contaminating stem cells with a capacity to 16 proliferate inappropriately after transplantation and/or differentiate into non-17 biliary cell types. Despite the association between organoids and adult stem 18 cells²⁶, we never observed the expression of hepatocyte or pancreatic 19 markers during our experiments either in vitro or after transplantation, 20 suggesting that the differentiation capacity of ECOs is limited to their lineage 21 of origin. Moreover, canonical WNT signaling, which is crucial for the 22 expansion of adult stem cell organoids²⁷ is blocked in our culture conditions 23 through the use of DKK-1 and further studies may be required to fully 24 elucidate the role of R-spondin in our system. Considered together, these 25

observations suggest that our culture system does not include a stem cell
population. However, we cannot completely exclude that these cells could
represent a biliary progenitor population based on their ability to selfpropagate and generate organoids from single cells.

Our system provides proof-of-principle for the application of primary cells in 5 regenerative medicine: however, the use of stem cells has been suggested as 6 an alternative for cell based therapy. Although we have recently established a 7 system for the generation of stem cell-derived cholangiocyte-like cells 8 (CLCs)⁹, there are considerable differences between ECOs and CLCs that 9 10 render ECOs better suited to regenerative therapies for extrahepatic biliary 11 injury. CLCs correspond to intrahepatic cholangiocytes, while ECOs represent extrahepatic biliary epithelium. These two cell types are distinct in terms of 12 embryological origin and disease involvement¹⁴. Furthermore, CLCs still 13 express fetal markers and therefore are more immature compared to ECOs 14 derived from primary cells⁹. Therefore, CLCs may require a period of 15 adjustment and further maturation in vivo, while mature, functional cells, such 16 as ECOs, are required for coping with biliary injury in the acute setting. 17 Finally, although hIPSCs provide a very good source of cells capable of 18 generating almost any tissue, fully differentiated CLCs cannot be expanded; 19 initial derivation/characterization of hIPSC lines remains time consuming; 20 while variability in capacity of differentiation still constitutes a challenge. ECOs 21 can be derived in less than 24 hours with a very high efficiency and can be 22 expanded for multiple passages without losing their original characteristics. 23 Consequently, ECOs are comparable to CLCs in terms of scalability, while 24

- 1 their mature phenotype provides a unique advantage for regenerative
- 2 medicine applications in the context of tissue repair.

In conclusion, our results open up novel avenues for the use of extrahepatic
primary biliary tissue as a novel platform for in vitro studies, disease modeling
and cell based therapy applications.

6

7 Accession codes

- 8 Accession number for microarray data: E-MTAB-4591.
- 9

10 Data availability statement

- 11 The microarray data are open access and available online on ArrayExpress
- 12 (https://www.ebi.ac.uk/arrayexpress/)

Acknowledgements: This work was funded by ERC starting grant Relieve 1 IMDs (LV, NRFH), the Cambridge Hospitals National Institute for Health 2 Research Biomedical Research Center (LV, NRFH, SaS, FS.), the Evelyn 3 trust (NH) and the EU Fp7 grant TissuGEN (MCDB) and supported in part by 4 the Intramural Research Program of the NIH/NIAID (RLG, CAR). FS has been 5 supported by an Addenbrooke's Charitable Trust Clinical Research Training 6 7 Fellowship and a joint MRC-Sparks Clinical Research Training Fellowship. AWJ and AEM acknowledge the support from EPSRC (EP/L504920/1) and an 8 9 Engineering for Clinical Practice Grant from the Department of Engineering, University of Cambridge. JB was supported by a BHF Studentship (Grant 10 FS/13/65/30441). 11

The authors would like to thank J Skepper, L Carter and the University of 12 Cambridge Advanced Imaging Centre for their help with electron microscopy; 13 E Farnell and the University of Cambridge, Cambridge Genomic Services for 14 15 their help with microarray data processing and analysis; A Petrunkina and the NIHR Cambridge BRC Cell Phenotyping Hub for their help with cell sorting; K 16 MRC MDU 17 Burling and the Mouse Biochemistry Laboratory [MRC MC UU 12012/5] for processing mouse serum samples; R El-Khairi 18 for her help with IF images, R Grandy for their help with providing relevant 19 20 references, the Cambridge Biorepository for Translational Medicine for the provision of human tissue used in the study and Mr B McLeod for IT support. 21 The monoclonal antibody TROMA-III developed by R Kemler was obtained 22 from the Developmental Studies Hybridoma Bank, created by the NICHD of 23 the NIH and maintained at The University of Iowa, Department of Biology, 24 lowa City, IA 52242. 25

1

Author Contributions: FS: Design and concept of study, execution of 2 experiments and data acquisition, development of protocols and validation, 3 collection and interpretation of data, production of figures, manuscript writing, 4 editing and final approval of manuscript; AWJ: Conception of the technique, 5 scaffold design and generation of densified collagen tubular scaffolds; OCT: 6 7 animal experiments including kidney capsule injections; cell culture, provision and harvesting of mouse tissue; StS: Magnetic Resonance Imaging (MRI); 8 9 EMG, SSU: MRI review and reporting; RLG: Animal experiments, IF, tissue histology; MCDB: Cell culture, generation of viral particles, viral transduction, 10 generation of GMP-ECOs; NLB, LV: Animal experiments; MJGV, PM: 11 12 Bioinformatics analyses; DO: Flow cytometry analyses; LY: Western blot analyses; AR: IF and QPCR analyses and provision of positive controls for IF 13 and QPCR; AB: Flow cytometry analyses, bioinformatics support; JB: Tissue 14 15 histology, IF; MarZ: Scaffold preparation; MTP: Generation of viral particles, viral transduction, generation of GMP-ECOs; MP: Generation of viral particles; 16 GMS: scaffold generation; PMM,KES: maintenance and provision of fibroblast 17 controls; NP: tissue culture; NG, CAR: Harvesting and preparation of primary 18 tissue; IS: Karyotyping, CGH analyses; SD: Histology review and reporting; 19 20 WS, JC, KBJ, MatZ, SaS, WTHG, GJA, SEB, TW, THK, EM: critical revision of the manuscript for important intellectual content. NRFH: Design and 21 concept of study, early study supervision AEM: Scaffold design, critical 22 23 revision of the manuscript for important intellectual content. KSP: Primary tissue provision, animal experiments, design and concept of study, study 24 supervision, interpretation of data, editing and final approval of manuscript. 25

- 1 LV: Design and concept of study, study supervision, interpretation of data,
- 2 editing and final approval of manuscript.
- 3
- 4 **Conflict of financial interests statement:** LV is a founder and shareholder
- 5 of DefiniGEN. The remaining authors have nothing to disclose.

1 References

2	1.	Murray, K. F. & Carithers, R. L. AASLD practice guidelines: Evaluation
3		of the patient for liver transplantation. Hepatology 41, 1407–1432
4		(2005).
5	2.	Perkins, J. D. Are we reporting the same thing?: Comments. Liver
6		<i>Transplant.</i> 13, 465–466 (2007).
7	3.	Skaro, A. I. et al. The impact of ischemic cholangiopathy in liver
8		transplantation using donors after cardiac death: The untold story.
9		Surgery 146 , 543–553 (2009).
10	4.	Enestvedt, C. K. et al. Biliary complications adversely affect patient and
11		graft survival after liver retransplantation. Liver Transpl. 19, 965–72
12		(2013).
13	5.	Gallo, A. & Esquivel, C. O. Current options for management of biliary
14		atresia. Pediatr. Transplant. 17, 95–98 (2013).
15	6.	Felder, S. I. et al. Hepaticojejunostomy using short-limb Roux-en-Y
16		reconstruction. JAMA Surg 148, 253–7-8 (2013).
17	7.	Sampaziotis, F., Segeritz, CP. & Vallier, L. Potential of human induced
18		pluripotent stem cells in studies of liver disease. Hepatology 62, 303-
19		311 (2015).
20	8.	Kanno, N., LeSage, G., Glaser, S., Alvaro, D. & Alpini, G. Functional
21		heterogeneity of the intrahepatic biliary epithelium. Hepatology 31, 555-
22		61 (2000).
23	9.	Sampaziotis, F. et al. Cholangiocytes derived from human induced

1		pluripotent stem cells for disease modeling and drug validation. Nat.
2		<i>Biotechnol.</i> 1–11 (2015). doi:10.1038/nbt.3275
3	10.	Sampaziotis, F. et al. Directed differentiation of human induced
4		pluripotent stem cells into functional cholangiocyte-like cells. Nat.
5		Protoc. 12, 814–827 (2017).
6	11.	LeSage, G., Glaser, S. & Alpini, G. Regulation of cholangiocyte
7		proliferation. <i>Liver</i> 21 , 73–80 (2001).
8	12.	Huch, M. et al. Long-Term Culture of Genome-Stable Bipotent Stem
9		Cells from Adult Human Liver. Cell 160, 299–312 (2014).
10	13.	Masyuk, A. I., Masyuk, T. V & LaRusso, N. F. Cholangiocyte primary
11		cilia in liver health and disease. Dev. Dyn. 237, 2007–12 (2008).
12	14.	Tabibian, J. H., Masyuk, A. I., Masyuk, T. V., O'Hara, S. P. & LaRusso,
13		N. F. Physiology of cholangiocytes. Compr. Physiol. 3, 541–565 (2013).
14	15.	Cízková, D., Morký, J., Micuda, S., Osterreicher, J. & Martínková, J.
15		Expression of MRP2 and MDR1 transporters and other hepatic markers
16		in rat and human liver and in WRL 68 cell line. Physiol. Res. 54, 419–28
17		(2005).
18	16.	Gigliozzi, A. et al. Molecular identification and functional
19		characterization of Mdr1a in rat cholangiocytes. Gastroenterology 119,
20		1113–22 (2000).
21	17.	Xia, X., Francis, H., Glaser, S., Alpini, G. & LeSage, G. Bile acid
22		interactions with cholangiocytes. World J. Gastroenterol. 12, 3553-63
23		(2006).

1	18.	Caperna, T. J., Blomberg, L. A., Garrett, W. M. & Talbot, N. C. Culture
2		of porcine hepatocytes or bile duct epithelial cells by inductive serum-
3		free media. In Vitro Cell. Dev. Biol. Anim. 47, 218–33 (2011).
4	19.	Marinelli, R. A. et al. Secretin induces the apical insertion of aquaporin-
5		1 water channels in rat cholangiocytes. Am. J. Physiol. 276, G280-6
6		(1999).
7	20.	Gong, AY. et al. Somatostatin stimulates ductal bile absorption and
8		inhibits ductal bile secretion in mice via SSTR2 on cholangiocytes. Am.
9		J. Physiol. Cell Physiol. 284, C1205-14 (2003).
10	21.	Ito, M. et al. NOD/SCID/gamma(c)(null) mouse: an excellent recipient
11		mouse model for engraftment of human cells. Blood 100, 3175–82
12		(2002).
13	22.	Chan, B. P. & Leong, K. W. Scaffolding in tissue engineering: general
14		approaches and tissue-specific considerations. Eur. Spine J. 17, 467–
15		479 (2008).
16	23.	Cheung, HY., Lau, KT., Lu, TP. & Hui, D. A critical review on
17		polymer-based bio-engineered materials for scaffold development.
18		Compos. Part B Eng. 38, 291–300 (2007).
19	24.	Jabłonska, B. End-to-end ductal anastomosis in biliary reconstruction:
20		indications and limitations. Can. J. Surg. 57, 271–277 (2014).
21	25.	Gjorevski, N. et al. Designer matrices for intestinal stem cell and
22		organoid culture. Nature 539, 560–564 (2016).
23	26.	Koo, B. K. & Clevers, H. Stem cells marked by the r-spondin receptor

1		LGR5. Gastroenterology 147, 289–302 (2014).
2	27.	Farin, H. F., Van Es, J. H. & Clevers, H. Redundant sources of Wnt
3		regulate intestinal stem cells and promote formation of paneth cells.
4		Gastroenterology 143 , 1518–1529.e7 (2012).
5		
6		

1 Figure Legends

2

3 Figure 1

Derivation and characterization of Extrahepatic Cholangiocyte Organoids 4 (ECOs). (a) Schematic representation of the method used for the derivation of 5 ECOs. (b) Quantitative real time PCR (QPCR) confirming the expression of 6 biliary markers in Passage 1 (P1), Passage 10 (P10) and Passage 20 (P20) 7 ECOs compared to freshly isolated Primary Cholangiocytes (PC) and 8 Embryonic Stem (ES) cells used as a negative control, n=4 ECO lines. 9 10 Center line, median; box, interguartile range (IQR); whiskers, range (minimum 11 to maximum). Values are relative to the housekeeping gene Hydroxymethylbilane Synthase (HMBS) (c) Immunofluorescence (IF) 12 analyses confirming the expression of biliary markers in ECO organoids. 13 Scale bars: 100 µm. Single channel and higher magnification images are 14 provided in Supplementary Fig 3. (d) Euclidean hierarchical clustering 15 analysis comparing the transcriptome of primary cholangiocytes (Primary), 16 passage 20 ECOs (ECO), hIPSC-derived intrahepatic cholangiocyte-like-cells 17 (iChoLC), ES cells (ES) and hepatocytes (HEP). For each probe, standard 18 scores (z-scores) indicate the differential expression measured in number of 19 standard deviations from the average level across all the samples. Clusters of 20 genes expressed in ECOs, primary cholangiocytes or both cell types are 21 indicated. GO analyses for each cluster are provided in Supplementary Fig. 22 7e. The data corresponds to 3 ECO lines. 23

24

1 Figure 2

2 Functional characterization of ECO organoids. (a) Fluorescence images demonstrating secretion of the MDR1 fluorescent substrate rhodamine 123 in 3 the lumen of ECOs, which is inhibited by the MDR1 inhibitor verapamil. Scale 4 bars: 100 µm. (b) Fluorescence intensity along the white line in (a). (c) Mean 5 intraluminal fluorescence intensity normalized to background in freshly plated 6 Primary Cholangiocytes (Rho PC), Passage 20 ECOs (Rho P20) and P20 7 ECOs treated with verapamil (Ver). Error bars, Standard Deviation (SD); 8 n=1565 measurements in total. Asterisks (****) indicate statistical significance 9 10 (P<0.001, Kruskal-Wallis test with Dunn's correction for multiple comparisons) 11 (d) Luminal extrusion of the fluorescent bile acid CLF compared to controls loaded with FITC, confirming bile acid transfer. Scale bars: 100 µm. (e) 12 Fluorescence intensity along the white line in (d). (f) Mean intra-luminal 13 fluorescence intensity normalized over background. n=1947 14 total measurements. Error bars, SD; asterisks as in (c). (g) ALP staining of ECOs. 15 Scale bars: Light microscopy: 500 µm, Whole well images: 1 cm. (h) Mean 16 GGT activity of P20 ECOs vs. PCs; error bars, SD; n=3, asterisks as in (c); 17 18 one-way ANOVA with Dunnett's correction for multiple comparisons. (i,j) Mean diameter measurements (i) and live images (i) of ECOs treated with 19 secretin or secretin and somatostatin, n=8. Error bars, SD; ***P<0.001; 20 #P>0.05 (Kruskal-Wallis test with Dunn's correction for multiple comparisons). 21 (a-j) Data representative of 3 different experiments. 22

23

24 Figure 3

ECOs dissociated to single cells (ECO-SCs) can populate biodegradable PGA 1 scaffolds. (a,b) Photographs of a PGA scaffold before (a) and after (b) 2 treatment with ECOs. Scale bars: 1 cm. (c) Light microscopy images of a 3 PGA scaffold populated with ECO-SCs. Red arrowheads: Fully populated 4 scaffold; black arrowheads: cells recruiting new PGA fibers; white 5 arrowheads: PGA fibers. Scale bars: 100µm. (d) Confocal microscopy images 6 7 demonstrating cell expansion at different time-points after seeding of GFPpositive ECO-SCs on a PGA scaffold. White lines indicate the position of PGA 8 9 fibers. Scale bars: 100µm. (e) IF demonstrating the expression of biliary markers and lack of EMT markers in ECO-SCs seeded on PGA scaffolds. 10 Scale bars: 100 µm (f) QPCR analyses demonstrating the expression of 11 12 biliary markers in ECOs before (ECOs) and after (scaffold) seeding on PGA scaffolds, n=4 ECO lines. Center line, median; box, interguartile range (IQR); 13 whiskers, range (minimum to maximum). Values are relative to the 14 15 housekeeping gene HMBS. (g) Mean ratio of CK7+/CK19+ and CK19+/Vimentin (VIM)+ cells in IF analyses similar to the image shown in (e). 16 Error bars represent SD; n=6. **P<0.01 (Mann-Whitney test). (h) Mean GGT 17 activity of ECO-SCs populating a PGA scaffold, n=4. Error bars represent SD. 18 ****P<0.001 (two-tailed t-test). (i) ALP staining of PGA scaffolds populated by 19 20 ECO-SCs. Scale bars: 500µm.

21

Figure 4

23 Biliary reconstruction in an extrahepatic biliary injury (EHBI) mouse model 24 using ECOs. (a) Schematic representation of the method used for biliary

reconstruction. (b) Kaplan-Meier survival analysis, demonstrating rescue of 1 EHBI mice following biliary reconstruction with ECO-populated scaffolds. 2 **P<0.01 (log-rank test). (c) Images of gallbladders reconstructed with 3 acellular PGA scaffolds (scaffold only), PGA scaffolds populated with ECOs 4 (transplanted) and native un-reconstructed gallbladder controls 5 (not transplanted), demonstrating full reconstruction with ECO populated scaffolds. 6 7 CD: cystic duct, CBD: common bile duct, CHD: common hepatic duct, F: fundus, A: anterior surface, P: posterior surface. Scale bars: 500 µm. (d) H&E 8 9 staining of the reconstructed gallbladders. L: lumen. Scale bars: 100 µm (e) IF analyses demonstrating the presence of GFP-positive ECOs expressing 10 biliary markers in the reconstructed gallbladders. L: lumen Scale bars: 100 11 um. Higher magnification images are provided in Supplementary Fig 12 (f.g) 12 FITC cholangiogram (n=1) (f) and MRCP images (n=2) (g) of reconstructed 13 (transplanted) vs. native control (not transplanted) gallbladders (GB) 14 15 demonstrating a patent lumen and unobstructed communication with the rest of the biliary tree. Scale bars: 1 mm. 16

17

18 Figure 5

ECOs can populate densified collagen tubular scaffolds. **(a)** Schematic representation of the method used for the generation of densified collagen tubular scaffolds. **(b)** Image of a densified collagen construct prior to tube excision. Scale bar, 500 μ m. **(c)** Maximum intensity projection image demonstrating a GFP+ ECO-populated tube after its generation. Scale bar; 30 μ m **(d)** Confocal microscopy image demonstrating lumen patency of an ECO-

populated collagen tube. Scale bar; 30 µm. (e) Images of a near confluent 1 GFP+ ECO-tube. Scale bar; 100 µm. (f) IF analyses demonstrating the 2 3 expression of biliary markers by ECOs following the generation of ECO-tubes. Scale bar; 100 µm. (g) QPCR analyses demonstrating the expression of 4 biliary markers before (ECOs) and after (Scaffold) the generation of ECO-5 populated collagen tubes. ES cells are used as a negative control, n=4 ECO 6 7 lines. Center line, median; box, interguartile range (IQR); whiskers, range (minimum to maximum). Values are relative to HMBS expression. (h, i) ECO-8 9 tubes exhibit ALP (h) and GGT (i) activity. Scale bars, 500µm; MEFs, Mouse Embryonic feeders used as negative control; Scaffold, ECO-populated, 10 densified collagen tubes; error bars, SD; n=3. 11

12

13 Figure 6

Bile duct replacement using ECO-populated densified collagen tubes. (a) 14 Schematic representation of the method used. (b) Postmortem images of 15 mice receiving ECO-populated collagen tubes (ECOs) vs. mice receiving 16 17 fibroblast-populated tubes (fibroblasts). Bile flow results in vellow pigmentation of ECO-tubes. The white color of the fibroblast conduit 18 19 combined with a dilated bile-filled (yellow color) Proximal Bile Duct (PBD) suggests luminal occlusion, resulting in bile leak (yellow peritoneal 20 pigmentation; white dashed line). SC: Collagen tubes/scaffolds; DBD: Distal 21 Bile Duct; scale bars 500 µm. (c) Images of a thin walled construct resembling 22 23 the native bile duct in animals receiving ECO-populated tubes vs. a thickened 24 construct with no distinguishable lumen in animals receiving fibroblast tubes.

Scale bars 500 µm. (d) QPCR using human-specific primers confirming the 1 expression of biliary markers by transplanted ECO-populated tubes (ECOs in 2 vivo) compared to cultured ECOs (ECOs in vitro) and mouse biliary tissue 3 used as a negative control, n=4 technical replicates. Center line, median; box, 4 interguartile range (IQR); whiskers, range (minimum to maximum). Values are 5 relative to HMBS expression. (e) H&E staining demonstrating the presence of 6 7 a biliary epithelium and a patent lumen in ECO-tubes but not fibroblast constructs. Scale bars 100 µm. (f) IF analyses demonstrating a GFP+/ CK19+ 8 9 epithelium lining the lumen of ECO-constructs, vs. obliteration of the lumen by 10 fibroblasts in fibroblast constructs. Scale bars 100 µm. (**q**) FITC cholangiogram, demonstrating lumen patency in ECO-tubes vs. lumen 11 12 occlusion in fibro-constructs. Scale bars: ECO, 100 µm; Fibroblasts, 500 µm (h) ALP activity is observed only in ECO-tubes, but not in fibroblast 13 constructs. Scale bars: ECO, 100 µm; Fibroblasts, 500 µm. 14

1 Online Methods

2 **Primary biliary tissue**

Primary biliary tissue (bile duct or gallbladder) was obtained from deceased organ donors from whom organs were being retrieved for transplantation. The gallbladder or a section of the bile duct was excised during the organ retrieval operation after obtaining informed consent from the donor's family (REC reference numbers: 12/EE/0253, NRES Committee East of England -Cambridge Central and 15/EE/0152 NRES Committee East of England -Cambridge South).

10 Isolation of primary cholangiocytes

Excised bile duct segments were placed in a 10 cm plate and washed once 11 with William's E medium (Gibco, Life Technologies). A longitudinal incision 12 was made along the wall of the excised bile duct segment exposing the lumen 13 and 10-15 ml of William's E medium were added to cover the tissue. The 14 15 luminal epithelium was subsequently scraped off using a surgical blade, while submerged in medium. The supernatant was collected and the tissue and 16 plate were washed 2-3 times with William's E medium to harvest any 17 remaining cells. The supernatant and washes were centrifuged at 444g for 4 18 minutes. The pellet was washed with William's E, re-centrifuged and the 19 supernatant was discarded (Figure 1a). 20

Excised gallbladders were placed in a 15 cm plate, a longitudinal incision was made along the wall of the excised gallbladder and the lumen was washed once with William's E medium (Gibco, Life Technologies). Cholangiocytes

were isolated and harvested following the method described above
 (Supplementary Fig 3a).

For isolation through brushings, an excised bile duct segment was placed in a
10 cm plate and cannulated using an ERCP brush. The lumen was brushed
10-20 times and the cells were harvested by washing the brush several times
in a falcon tube containing 40-50 ml of William's E medium (Supplementary
Fig 3b).

8 Generation and culture of ECOs

9 Isolated primary cholangiocytes were centrifuged at 444g for 4 minutes and re-suspended in a mixture of 66% matrigel (BD Biosciences, catalogue 10 number: 356237) and 33% William's E medium (Gibco, Life Technologies) 11 supplemented with 10mM nicotinamide (Sigma-Aldrich), 17mM sodium 12 bicarbonate (Sigma Aldrich), 0.2mM 2-Phospho-L-ascorbic acid trisodium salt 13 (Sigma-Aldrich), 6.3mM sodium pyruvate (Invitrogen), 14mM glucose (Sigma-14 Aldrich), 20mM HEPES (Invitrogen), ITS+ premix (BD Biosciences), 0.1µM 15 dexamethasone (R&D Systems), 2mM Glutamax (Invitrogen),100U/ml 16 17 penicillin per 100µg/ml streptomycin, 20ng/ml EGF (R&D Systems), 500ng/ml R-Spondin (R&D Systems) and 100ng/ml DKK-1 (R&D Systems). The cell 18 19 suspension was plated in 24-well plate format, at 50µl/well, so that a small 20 dome of matrigel was formed in the centre of each well and then incubated at 37°C for 10-30 minutes until it solidified. Subsequently, 1ml of William's E 21 medium with supplements was added. The culture medium was changed 22 23 every 48 hours.

To split the cells, the matrigel was digested by adding Cell Recovery Solution (Corning) for 30 minutes at 4°C. The resulting cell suspension was harvested, centrifuged at 444g for 4 minutes, washed once with William's E medium and re-suspended in 66% matrigel and 33% William's E medium with supplements, as described above.

All experiments were performed using passage 20 ECOs unless otherwisestated.

8 Cell line identity

Demographic data for donor corresponding to the each ECO lines is provided
in supplementary table 1. Following derivation ECO lines were authenticated
by matching their karyotype (Supplementary Fig. 4b) to the sex of the donor of
origin. The lines were tested on a regular basis and found to be negative for
mycoplasma contamination.

14 Immunofluorescence, RNA extraction and Quantitative Real Time PCR

IF, RNA extraction and QPCR were performed as previously described⁹. A complete list of the primary and secondary antibodies used is provided in supplementary table 3. A complete list of the primers used is provided in supplementary table 4.

All QPCR data are presented as the median, interquartile range (IQR) and range (minimum to maximum) of four independent ECO lines unless otherwise stated. Values are relative to the housekeeping gene Hydroxymethylbilane Synthase (*HMBS*).

All IF images were acquired using a Zeiss Axiovert 200M inverted microscope
 or a Zeiss LSM 700 confocal microscope. Imagej 1.48k software (Wayne

1 Rasband, NIHR, USA, <u>http://imagej.nih.gov/ij</u>) was used for image processing.

2 IF images are representative of 3 different experiments. IF images of
 3 reconstructed gallbladder sections are representative of 5 different animals.

4 Microarrays

RNA for microarray analysis was collected from 3 different ECO lines (n=3). 65 The RNA was assessed for concentration and quality using a SpectroStar 66 67 (BMG Labtech, Aylesbury, UK) and a Bioanalyser (Agilent Technologies, Cheadle, UK). Microarray experiments were performed at Cambridge 68 69 Genomic Services, University of Cambridge, using the HumanHT-12 v4 (Illumina, Chesterford, UK) according Expression BeadChip to the 70 manufacturer's instructions. Briefly, 200ng of Total RNA underwent linear 71 72 amplification using the Illumina TotalPrep RNA Amplification Kit (Life 73 Technologies, Paisley, UK) following the manufacturer's instructions. The concentration, purity and integrity of the resulting cRNA were measured by 74 75 SpectroStar and Bioanalyser. Finally cRNA was hybridised to the HumanHT-12 v4 BeadChip overnight followed by washing, staining and scanning using 76 the Bead Array Reader (Illumina). The microarray data are available on 77 ArrayExpress (Accession number: E-MTAB-4591). For reviewer access, 78 please use the following login details Username: Reviewer E-MTAB-4591 79 80 Password: rtllmbi0

81 Microarrays analysis

Raw data was loaded into R using the lumi package from bioconductor²⁸ and divided into subsets according to the groups being compared; only the samples involved in a given comparison are used. Subsets were then filtered to remove any non-expressed probes using the detection p-value from

Illumina. Across all samples probes for which the intensity values were not 1 statistically significantly different (P>0.01) from the negative controls were 2 removed from the analysis. Following filtering the data was transformed using 3 the Variance Stabilization Transformation²⁹ from lumi and then normalised to 4 remove technical variation between arrays using quantile normalisation. 5 Comparisons were performed using the limma package³⁰ with results 6 corrected for multiple testing using False Discovery Rate (FDR) correction. 7 Finally the quality of the data was assessed along with the correlations 8 9 between samples within groups.

Probes differentially expressed between HEP and ECOs representing the 10 aggregate transcriptional "signature" of ECOs were selected for Euclidean 11 12 hierarchical clustering using Perseus software (MaxQuant). Standard scores (z-scores) of the log2 normalized probe expression values across the different 13 conditions were calculated and used for this analysis. Heatmaps and Primary 14 Component Analysis (PCA) plots were generated using the MaxQuant 15 (http://www.perseus-framework.org/)³¹. Perseus software Functional 16 annotation and gene ontology analyses were performed on the genes 17 differentially expressed between PCs and ECOs (Figure 1d) using the 18 NIAID/NIH Database for Annotation, Visualization and Integrated Discovery 19 (DAVID) v6.8 (https://david.ncifcrf.gov/)^{32,33}. 20

21 Western Analysis

Total protein was extracted with lysis buffer (50mM Tris pH 8, 150mM NaCl,
0.1% SDS, 0.5% sodium deoxycholate, 1% Trition X-100 and protease and
phosphatase inhibitors). Protein concentrations were determined by BCA
Protein Assay Kit (Thermo Fisher Scientific) according to the manufacturer's

instructions. Samples were prepared for Western blot by adding 1x NuPAGE 1 LDS Sample Buffer with 1% ß-mercaptoethanol and incubated for 5 minutes 2 at 95°C. Protein (25 µg) was separated by 4-12% NuPAGE Bis-Tris protein 3 gels (Invitrogen) and transferred onto PVDF membranes (Bio-Rad). Proteins 4 were detected by probing with antibodies specific to Phospho-β-catenin 5 (Ser33/37/Thr41) (Cell Signalling Technology), Active-β-catenin (Millipore), 6 Total- β -catenin (R&D), α -tubulin (Sigma) followed by incubation with 7 horseradish peroxidase anti-mouse, anti-goat or anti-rabbit secondary 8 9 antibodies. Membranes were developed using Pierce ECL Western blotting substrate (Thermo Scientific) according to the manufacturer's instructions. 10

11 **Rho Kinase activity analyses**

Rho Kinase activity was measured using a commercially available kit (Cell
 Biolabs, STA-416) according to the manufacturer's instructions

14 Flow cytometry analyses

ECO organoids were harvested using Cell Recovery Solution (Corning) for 30 minutes at 4°C, centrifuged at 444g for 4 minutes and dissociated to single cells using TrypLETM Express (Gibco). The cells were subsequently fixed using 4% PFA for 20 minutes at 4°C. Cell staining and flow cytometry analyses were performed as previously described^{9,34}.

20 Karyotyping

ECO organoids were harvested using Cell Recovery Solution (Corning), dissociated to single cells as described above, plated in gelatin coated plates and cultured using William's E medium with supplements. When the cells were sub-confluent, usually after 72hrs, the cultures were incubated for 3-4 hours with William's E medium with supplements containing 0.1µg/ml

colcemid (Karyomax®, Gibco). The cells were then harvested using TrypsinEDTA (0.05%) (Gibco) for 4-5 minutes at 37°C, centrifuged at 344g for 5
minutes and re-suspended in 5mls of KCI hypotonic solution (0.055M). The
suspension was re-centrifuged at 344g for 5 minutes, 2 mls of a 3:1 100%
methanol:glacial acetic acid solution were added and slides were prepared as
previously described³⁵

7 Comparative Genomic Hybridization analyses

Genomic DNA was labeled using the BioPrime DNA Labeling Kit (Invitrogen),
according to the manufacturer's instructions and samples were hybridised to
Agilent Sureprint G3 unrestricted CGH ISCA 8x60K human genome arrays
following the manufacturer's protocol, as previously described³⁶. The data
was analysed using the Agilent CytoGenomics Software.

13 Rhodamine123 transport assay

The Rhodamine 123 transport assay was performed as previously described⁹ and images were acquired using a Zeiss LSM 700 confocal microscope. Fluorescence intensity was measured between the organoid interior and exterior and luminal fluorescence was normalized over the background of the extraluminal space. Each experiment was repeated in triplicate. Error bars represent SD.

20 Cholyl-Lysyl-Fluorescein transport assay

То achieve loading with Cholyl-Lysyl-Fluorescein (CLF, 21 Corning Incorporated), ECO organoids were split in 5µM of CLF and incubated at 37°C 22 23 for 30 minutes. Images were acquired using a Zeiss LSM 700 confocal microscope and fluorescence intensity was measured between the organoid 24 25 interior and exterior as described for the Rhodamine 123 transport assay. To

demonstrate that the changes in CLF fluorescence intensity observed were
secondary to active export of CLF from the organoid lumen, the experiment
was repeated with 5µM of unconjucated Fluorescein Isothiocyanate (FITC)
(Sigma-Aldrich) as a control. Fluorescence intensity measurements were
performed as described for the Rhodamine 123 transport assay. Each
experiment was repeated in triplicate. Error bars represent SD.

7 **GGT activity**

GGT activity was measured in triplicate using the MaxDiscovery[™] gammaGlutamyl Transferase (GGT) Enzymatic Assay Kit (Bioo scientific) based on
the manufacturer's instructions. Error bars represent SD.

11 Alkaline Phosphatase staining

Alkaline phosphatase was carried out using the BCIP/NBT Color
 Development Substrate (5-bromo-4-chloro-3-indolyl-phosphate/nitro blue
 tetrazolium) (Promega) according to the manufacturer's instructions.

15 **Response to Secretin and Somatostatin**

Responses to secretin and somatostatin were assessed as previously
 described⁹.

18 Generation of ECOs expressing Green Fluorescent Protein

EGFP expressing VSV-G pseudotyped, recombinant HIV-1 lentiviral particles were produced with an optimized second generation packaging system by transient co-transfection of three plasmids into HEK 293T cells (ATCC CRL-11268). EGFP expression is under control of a core EF1α-promoter. All plasmids were a gift from Didier Trono and obtained from addgene (pWPT-GFP #12255, psPAX2 #12260, pMD2.G, #12259). Viral infection of organoids was performed as previously described³⁷. Infected ECOs were expanded for 2

passages, harvested as described above for flow cytometry analyses and cell sorting by flow cytometry for GFP positive cells was performed. GFP expressing single cells were plated using our standard plating method and cultured in William's E medium with supplements for 1-2 weeks until fully grown ECO organoids developed.

6 Generation of ECO populated PGA scaffolds

1mm thick PolyGlycolic Acid (PGA) scaffolds with a density of 50mg/cc were used for all experiments. Prior to seeding cells, the PGA scaffolds were pretreated with a 1M NaOH for 10-30 seconds washed 3 times, decontaminated in a 70% ethanol solution for 30 minutes and then air-dried for another 30 minutes until all the ethanol had fully evaporated. All scaffolds were a gift from Dr Sanjay Sinha and obtained from Biomedical Structures (Biofelt).

ECOs were harvested and dissociated to single cells as previously described 13 for flow cytometry analyses. 5-10x10⁶ cells were re-suspended in 100 µl of 14 15 William's E medium with supplements, seeded on a scaffold surface area of 1cm² and incubated at 37°C for 30-60 minutes to allow the cells to attach to 16 the scaffold. The scaffolds were placed in wells of a 24-well plate and 17 checked at regular intervals during this period to ensure the medium did not 18 evaporate. If necessary, 10-20 µl of William's E medium with supplements 19 20 were added. After 1 hour, 2-3 mls of William's E medium with supplements were added to the wells and the medium was changed twice weekly. 21

22 Generation of densified collagen tubes

Densified collagen tubes were prepared using a novel approach. A 3D printed
chamber was fabricated, consisting of a funnel piece and a base plate. A
250µm thick metallic wire was mounted into the base plate and fed through

the centre of the funnel. Absorbent paper towels were compacted between 1 the two 3D printed parts, which were then screwed together. 5 mg mL⁻¹ 2 collagen gel solution, loaded with cells, was poured into the funnel and gelled 3 at 37°C for 30 min. After that time, the screws were loosened and, by placing 4 the 3D printed chambers at 37°C for 2-4h, water was drawn out of the 5 collagen gel. A cell-loaded densified collagen tube was thus formed with a 6 7 250µm lumen and a wall thickness of 30-100 µm, determined by the duration of the drying phase. Upon removal from the chamber, the tube was trimmed 8 9 for excess collagen and cut to the required length.

10 Culture of Human Mammary Epithelial Cells (HMECs)

HMECs and the required tissue culture consumables were purchased as a kit
 from Lonza (cat no. cat no. CC-2551B) and the cells were cultured according
 to the supplier's instructions

14 Animal experiments

All animal experiments were performed in accordance with UK Home Office regulations (UK Home Office Project License numbers PPL 80/2638 and PPL 70/8702). Immunodeficient NOD.Cg-Prkdc^{scid} II2rg^{tm1WjI}/SzJ (NSG) mice which lack B, T and NK lymphocytes³⁸ were bred in-house with food and water available ad libitum pre- and post-procedures. A mix of male and female animals were used, aged approximately 6-8 weeks. All the ECO-constructs used were populated with ECOs derived from the common bile duct.

22 Generation of Extra-Hepatic Biliary Injury (EHBI) mouse model

To generate a model of extrahepatic biliary injury, midline laparotomy was performed and the gallbladder was first mobilized by dividing the ligamentous attachment connecting its fundus to the anterior abdominal wall under

isoflurane general anesthesia. A longitudinal incision was then made along
2/3 of the length of the gallbladder, from the fundus towards Hartmann's
pouch (neck of gallbladder).

4 Biliary reconstruction in EHBI mice

5 To reconstruct the gallbladder, a scaffold section measuring approximately 1 x 6 1 mm (seeded with ECOs or without ECOs in controls) was sutured as a 7 'patch' to close the defect using 4 – 6 interrupted 10'0 non-absorbable nylon 8 sutures under 40x magnification. The laparotomy was closed in two layers 9 with continuous 5'0 absorbable Vicryl sutures. The animals were given 10 buprenorphine (temgesic 0.1 mg/kg) analgesia as a bolus and observed every 11 15 minutes in individual cages until fully recovered.

8 animals underwent biliary reconstruction using an ECO-populated scaffold. All animals survived up to 104 days without complications and were culled electively for further analyses. Two control experiments were performed, where the animals underwent biliary reconstruction using acellular scaffolds. Both animals died within 24 hours from bile leak, therefore no further control experiments were performed to minimize animal discomfort.

18 Bile duct replacement

The native common bile duct was divided and a short segment excised. The populated densified collagen tube was anastomosed end-to-end, using interrupted 10'0 nylon sutures, between the divided proximal and distal common bile duct. A length of 5'0 nylon suture material (diameter 100 μ m) was inserted into the collagen tube and fed into the proximal and distal common bile duct to ensure patency of the lumen during the anastomosis. After the anastomosis was complete, the 5'0 suture was pushed into the

duodenum through the distal bile duct and was removed through an incision in 1 the duodenum, which was then closed with interrupted 10'0 nylon sutures. 2 3 Lumen patency was assessed at the time of transplantation through light microscopy and cannulation of the lumen with a 5'0 non-absorbable suture. 4 Transplantation was abandoned as futile in case of fully occluded tubes due 5 to cell infiltration. These events were considered construct/tube failure rather 6 7 than surgical complications and therefore were not censored in the survival 8 analysis.

9 **Bile duct ligation**

10 C57BL/6 mice were purchased from The Jackson Laboratory (Bar Harbor, ME). The mice were housed and bred in a Minimal Disease Unit at the animal 11 facility at Oslo University Hospital, Rikshospitalet, Oslo. All experiments were 12 performed on male mice between 8 and 12 weeks of age. A median 13 laparotomy was performed, the common bile duct exposed and ligated close 14 15 to the junction of the hepatic bile ducts. Sham operated mice underwent the same procedure without ligation. Serum was harvested after 5 days. Alanine 16 transaminase (ALT), aspartate transaminase (AST) and alkaline phosphatase 17 (ALP) were measured in serum using an ADVIA 1800 (Siemens) at The 18 Central Laboratory, Norwegian School of Veterinary Science. All animal 19 experiments were approved by the Norwegian Food Safety Authority (project 20 license no FOTS 8210/15) and all animals received human care in line with 21 22 "Guide for the Care and Use of Laboratory Animals" (National Institutes of Health Publication, 8th Edition, 2011). 23

24 Blood sample collection

Blood was taken using a 23g needles directly from the inferior vena cava
under terminal anaesthesia at the time the animals were electively culled and
transferred into 1.5ml Eppendorf tubes for further processing.

4 Blood sample processing

5 The blood samples were routinely processed by the University of Cambridge 6 Core biochemical assay laboratory (CBAL). All of the sample analysis was 7 performed on a Siemens Dimension EXL analyzer using reagents and assay 8 protocols supplied by Siemens.

9 Light microscopy imaging

Light microscopy images of excised reconstructed gallbladders were acquired using a Leica MZFLIII fluorescence dissecting microscope. The images are representative of 5 animals.

13 Cryosectioning and Histology

Excised gallbladders were fixed in 4% PFA, immersed in sucrose solution overnight, mounted in optimal cutting temperature (OCT) compound and stored at -80°C until sectioning. Sections were cut to a thickness of 10µm using a cryostat microtome and mounted on microscopy slides for further analysis

19 Haematoxylin and Eosin (H&E) Staining

H&E staining was performed using Sigma-Aldrich reagents according to the manufacturer's instructions. Briefly, tissue sections were hydrated, treated with Meyer's Haematoxylin solution for 5 minutes (Sigma-Aldrich), washed with warm tap water for 15 minutes, placed in distilled water for 30-60 seconds and treated with eosin solution (Sigma-Aldrich) for 30-60 seconds.

The sections were subsequently dehydrated and mounted using the Eukitt® quick-hardening mounting medium (Sigma-Aldrich). Histology sections were reviewed by an independent histopathologist with a special interest in hepatobiliary histology (SD).

5 TUNEL assay

The TUNEL assay was performed using a commercially available kit (abcam,
ab66110) according to the manufacturer's instructions.

8 Fluorescein Isothiocyanate (FITC) cholangiography

9 In situ FITC cholangiography was performed in sacrificed animals after 10 dissection of the gallbladder free from the adherent liver lobes, but before 11 surgical interruption of the extrahepatic biliary tree. The distal bile duct was 12 cannulated with a 23½ gauge needle and FITC injected retrogradely into the 13 gallbladder and images taken under a fluorescent microscope.

14 Magnetic Resonance Cholangio-Pancreatography (MRCP)

Magnetic resonance cholangio-pancreatography was performed after sacrifice of the animals. MRCP was performed at 4.7T using a Bruker BioSpec 47/40 system. A rapid acquisition with relaxation enhancement sequence was used with an echo train length of 40 echoes at 9.5ms intervals, a repetition time of 1000ms, field of view 5.84×4.18×4.18cm³ with a matrix of 256×180×180 yielding an isotropic resolution of 230 µm. The actively-decoupled fourchannel mouse cardiac array provided by Bruker was used for imaging.

For the second mouse imaged, for higher signal to noise ratio to give improved visualisation of the biliary ducts a two-dimensional sequence was used with slightly varied parameters (24 spaced echoes at 11ms intervals to give an effective echo time of 110ms; repetition time 5741ms; matrix size of

256×256; field of view of 4.33×5.35cm² yielding a planar resolution of
170×200µm²). Fifteen slices were acquired coronally through the liver and gall
bladder with a thickness of 0.6mm. For this acquisition, a volume coil was
used to reduce the impact of radiofrequency inhomogeneity.

To examine the biliary ducts and gall bladder, images were prepared by
maximum intensity projections. Structural imaging to rule out neoplastic
growths was performed using a T1-weighted 3D FLASH (fast low-angle shot)
sequence with a flip angle of 25°, repetition time of 14ms and an echo time of
7ms. The matrix was 512×256×256 with a field of view of 5.12×2.56×2.56cm³
for a final isotropic resolution of 100 µm.

11 The MRCP images were reviewed by 2 independent radiologists with a 12 special interest in hepatobiliary radiology (EMG, SU).

13 Statistical analyses

All statistical analyses were performed using GraphPad Prism 6. For small 14 15 sample sizes where descriptive statistics are not appropriate, individual data points were plotted. For comparison between 2 mean values a 2-sided 16 student's t-test was used to calculate statistical significance. The normal 17 distribution of our values was confirmed using the D'Agostino & Pearson 18 omnibus normality test where appropriate. Variance between samples was 19 20 tested using the Brown-Forsythe test. For comparing multiple groups to a reference group one-way ANOVA with Dunnett correction for multiple 21 comparisons was used between groups with equal variance, while the 22 23 Kruskal-Wallis test with Dunn's correction for multiple comparisons was applied for groups with unequal variance. Survival was compared using log-24 25 rank (Mantel-Cox) tests. Where the number of replicates (n) is given this

refers to ECO lines or number of different animals unless otherwise stated.
 Further details of the statistical analyses performed are provided in
 Supplementary table 5.

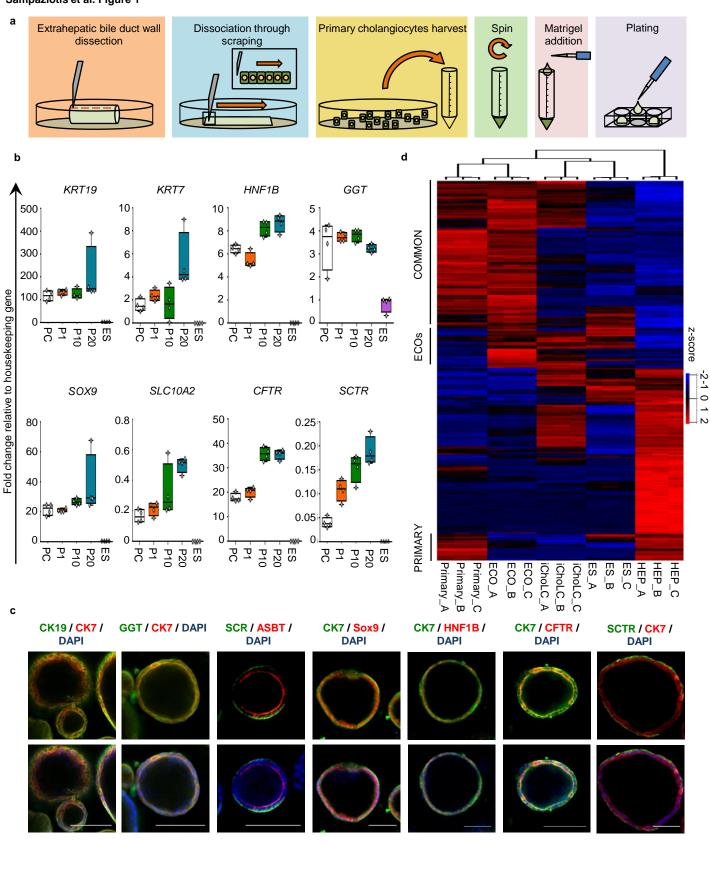
For animal experiments, group sizes were estimated based on previous study 4 variance. Final animal group sizes were chosen to allow elective culling at 5 different time point while maintaining n>4 animals surviving past 30 days to 6 7 ensure reproducibility. No statistical methods were used to calculate sample size. No formal randomization method was used to assign animals to study 8 groups. However; littermate animals from a cage were randomly assigned to 9 10 experimental or control groups by a technician not involved in the study. No 11 animals were excluded from the analysis. No blinding was used when only one group of animals survived for radiology imaging. In cases, such as 12 13 gallbladders reconstructed with fibroblasts vs. ECOs where more than one groups survived to be imaged, both radiologists reviewing the images (EG 14 and SU) where blinded to the method of reconstruction. 15

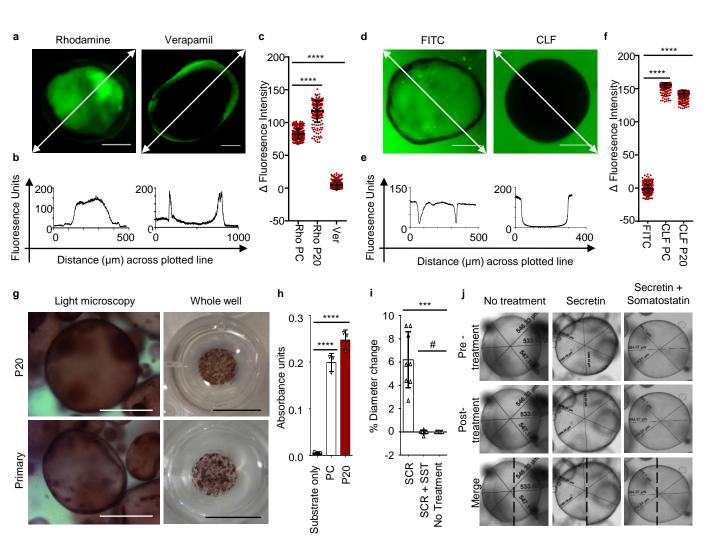
1 References

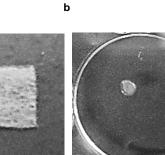
3	28.	Du, P., Kibbe, W. a & Lin, S. M. lumi: a pipeline for processing Illumina
4		microarray. Bioinformatics 24, 1547–8 (2008).
5	29.	Lin, S. M., Du, P., Huber, W. & Kibbe, W. A. Model-based variance-
6		stabilizing transformation for Illumina microarray data. Nucleic Acids
7		Res. 36 , (2008).
8	30.	Smyth, G. K. Linear models and empirical bayes methods for assessing
9		differential expression in microarray experiments. Stat Appl Genet Mol
10		Biol 3, Article3-Article3 (2004).
11	31.	Tyanova, S. et al. The Perseus computational platform for
12		comprehensive analysis of (prote)omics data. Nat. Methods 13, 731–40
13		(2016).
14	32.	Huang, D. W., Sherman, B. T. & Lempicki, R. A. Systematic and
15		integrative analysis of large gene lists using DAVID bioinformatics
16		resources. Nat. Protoc. 4, 44–57 (2008).
17	33.	Huang, D. W., Sherman, B. T. & Lempicki, R. A. Bioinformatics
18		enrichment tools: paths toward the comprehensive functional analysis of
19		large gene lists. Nucleic Acids Res. 37, 1–13 (2009).
20	34.	Bertero, A. et al. Activin/Nodal signaling and NANOG orchestrate
21		human embryonic stem cell fate decisions by controlling the H3K4me3
22		chromatin mark. <i>Genes Dev.</i> 29, 702–17 (2015).
23	35.	Campos, P. B., Sartore, R. C., Abdalla, S. N. & Rehen, S. K.
24		Chromosomal spread preparation of human embryonic stem cells for

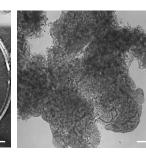
1		karyotyping. J. Vis. Exp. 4–7 (2009). doi:10.3791/1512
2	36.	Hannan, N. R. F. et al. Generation of multipotent foregut stem cells from
3		human pluripotent stem cells. Stem Cell Reports 1, 293–306 (2013).
4	37.	Koo, BK., Sasselli, V. & Clevers, H. Retroviral gene expression control
5		in primary organoid cultures. Curr. Protoc. Stem Cell Biol. 27, Unit 5A.6.
6		(2013).
7	38.	Shultz, L. D. et al. Human lymphoid and myeloid cell development in
8		NOD/LtSz-scid IL2R gamma null mice engrafted with mobilized human
9		hemopoietic stem cells. J. Immunol. 174, 6477–6489 (2005).
10		
11		
12		

Sampaziotis et al. Figure 1

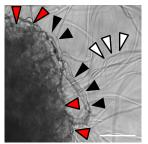


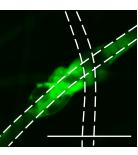


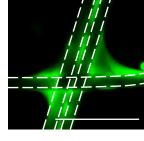


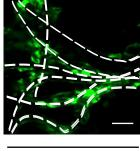


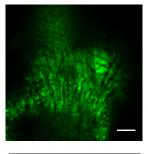
С







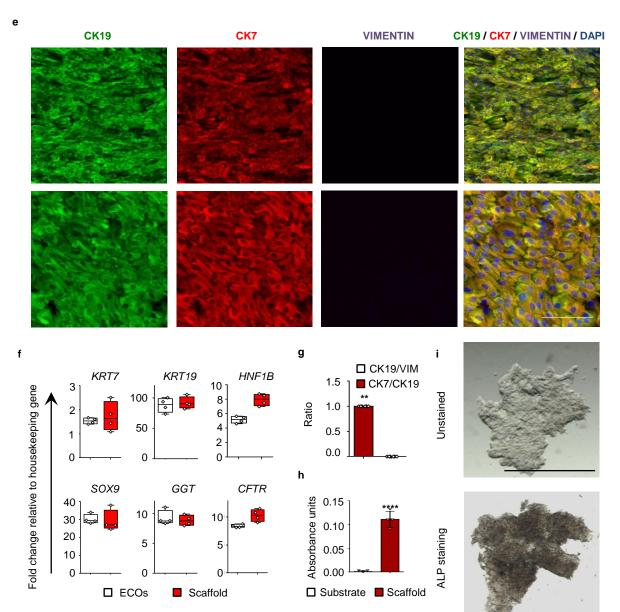


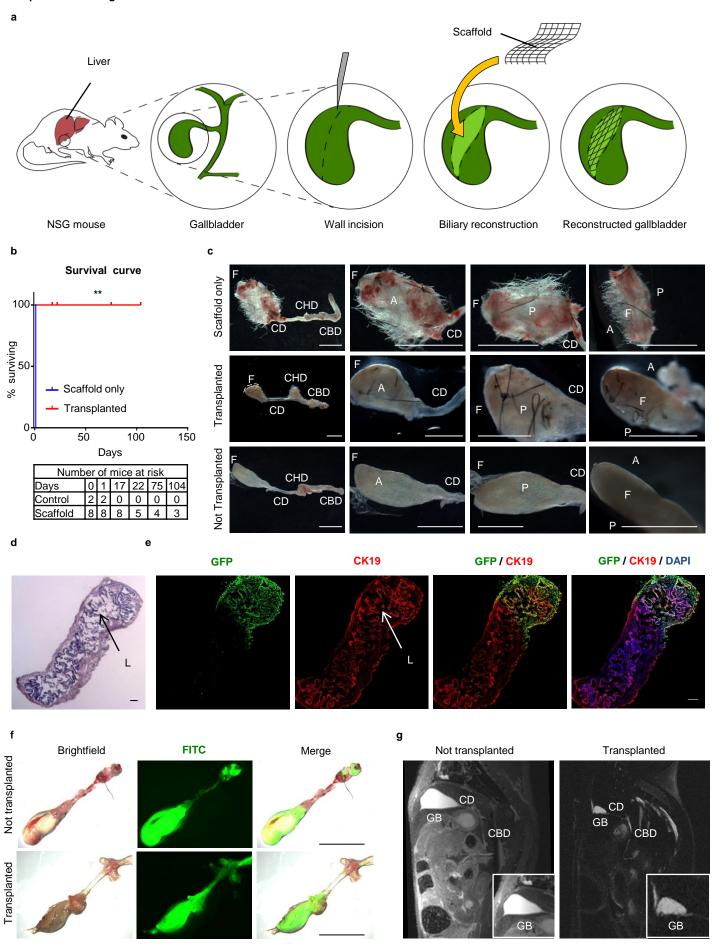


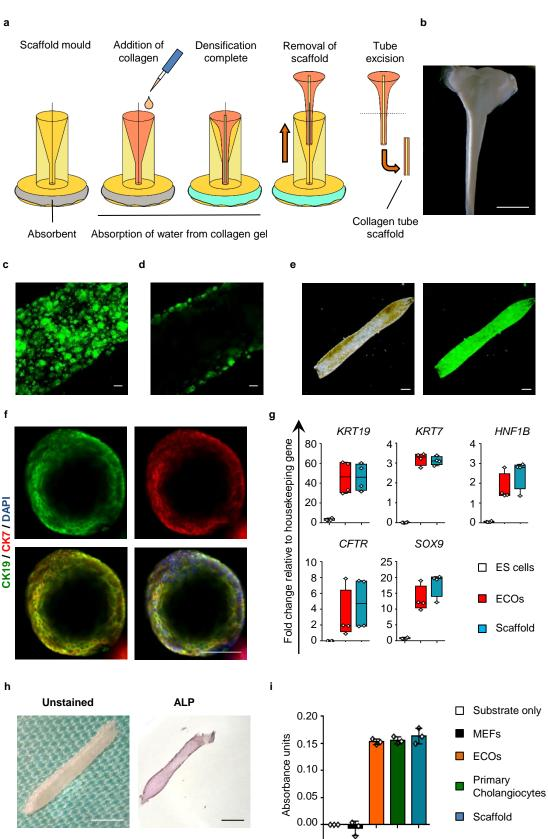
48hrs

2 weeks

4 weeks







CK19 / CK7 / DAPI

Sampaziotis et al. Figure 6

